Time-Resolved Resonance Raman Spectroscopy and Density Functional Study of 2-Fluorenylnitrene and Its Dehydroazepine Products

Shing Yau Ong,[a] Peizhi Zhu,[a] Yuen Fan Poon,[a] King Hung Leung,[a] Wei-Hai Fang,[a, b] and David Lee Phillips*[a]

Abstract: We report time-resolved resonance Raman spectra for 2-fluorenylnitrene and its dehydroazepine products acquired after photolysis of 2-fluorenylnitrene in acetonitrile. The experimental Raman band frequencies exhibit good agreement with the calculated vibrational frequencies from UBPW91/cc-PVDZ density functional calculations for the singlet and triplet states of the 2-fluorenylnitrene as well as BPW91/cc-PVDZ calculations for the two dehydroazepine ring-expansion product species. The decay of the 2-fluorenylnitrene Raman signal and the appearance of the dehydroazepine products suggest the presence of an intermediate species (probably an azirine) that does not absorb very much at the 416 nm probe wavelength used in the time-resolved resonance Raman experiments. Comparison of the singlet 2-fluorenylnitrene species with the singlet 2-fluorenylnitrenium ion species indicates that protonation of the nitrene to give the nitrenium ion leads to a significant enhancement of the cyclohexadienyl character of the phenyl rings without much change of the C–N bond length.

Keywords: arylnitrenes · arylnitrenium ions · density functional calculations · Raman spectroscopy

Introduction

There has been a great deal of interest in the photochemistry of aryl azides,[1–59] and a better understanding of their reaction mechanisms has proceeded rapidly over the past decade with the application of laser flash-photolysis techniques to directly probe their reaction intermediates and photoproducts. Photolysis of aryl azides in solution typically leads to the formation of a singlet nitrene species and a nitrogen molecule. The singlet nitrene may then undergo very rapid ring expansion to produce ketenimines (dehydroazepine), which can be trapped by nucleophiles. In some cases (e.g., singlet 2-pyrimidylnitrene),[55] the singlet nitrene species may decay mainly by intersystem crossing to the triplet nitrene species. The chemistry and reaction mechanisms of singlet phenyl nitrene has been extensively studied and well characterized.[7, 8, 18, 20, 21, 42–46, 52–54] Singlet phenyl nitrene has been directly observed at room temperature[44, 45] and has a short lifetime of ≈ 1 ns that is mainly caused by the fast ring-expansion reaction ($E_a = 2-3$ kcal mol^{-1}). The lifetime of the singlet nitrenes can become substantially longer when various substituents are used.[16–18, 22–25, 29, 40, 55, 57] For example, photolysis of polyfluorinated phenyl azides in acetonitrile have been shown to produce singlet nitrenes with lifetimes of tens to hundreds of nanoseconds,[40] because the ring-expansion reaction becomes slower with a higher activation barrier.[16–18, 22–25, 29, 40, 55, 57] These longer lived singlet nitrene species can be trapped more easily by nucleophiles, such as diethylamine, pyridine, and tetramethylethylene. Some of these longer lived singlet nitrenes have also been found to undergo fast protonation reactions to produce singlet nitrenium ions.[26, 28, 31–37, 40, 47, 48] While a great deal has been learned about the chemistry and reaction mechanisms of arylnitrenes, there are few reports of direct vibrational mode-specific characterization of singlet or triplet arylnitrenes in room temperature solutions.

In this paper, we report a time-resolved resonance Raman spectroscopic study of arylnitrenes produced following ultraviolet photolysis of 2-fluorenylnitrene in acetonitrile. To our knowledge, these are the first time-resolved resonance Raman spectra obtained for photochemically generated arylnitrenes in room-temperature solutions. We observe a number of vibrational Raman bands in the time-resolved spectra and their vibrational frequencies exhibit good agreement with those calculated from density functional calculations for singlet (and triplet) 2-fluorenylnitrene and their ring-

[a] D. L. Phillips, S. Y. Ong, P. Zhu, Y. F. Poon, K. H. Leung, W.-H. Fang
Department of Chemistry, The University of Hong Kong
Pokfulam Road, Hong Kong S.A.R. (P. R. China)
Fax: (+852)-2857-1586
E-mail: phillips@hkucc.hku.hk

[b] W.-H. Fang
Department of Chemistry, Beijing Normal University
Beijing 100875 (P. R. China)

Supporting information for this article is available on the WWW under http://www.wiley-vch.de/home/chemistry/ or from the author.

  0947-6539/02/0809-2163 $ 20.00+.50/0

expansion dehyroazepine products. The experimental Raman vibrational frequencies (in conjunction with density functional computational results) provide experimental evidence that these singlet (and/or triplet) arylnitrenes have noticeable cyclohexadienyl character. Comparison of the singlet nitrene species with their corresponding singlet nitrenium ion species indicates that the degree of cyclohexadienyl character increases noticeably when the singlet arylnitrenium ion is formed. The resonance Raman bands of 2-fluorenylnitrene decrease in intensity with no immediate formation of the dehydroazepine products that can be observed on the microsecond timescale. This suggests there is a dark intermediate (probably an azirine species) formed from the 2-fluorenylnitrene precursor which then reacts further to produce the dehydroazepine products.

Results and Discussion

Figure 1 presents the 416 nm transient resonance Raman spectra obtained 10 ns after 309 nm photolysis of 2-fluorenylnitrene in acetonitrile (top) and in a mixed solvent system of 75 % water/25 % acetonitrile by volume (bottom). Figure 2 displays the 416 nm time-resolved resonance Raman spectra obtained 10 ns, 50 ns, 100 ns, 500 ns, 5 μs, and 10 μs after 266 nm photolysis of 2-fluorenylnitrene in acetonitrile. Tables 1 and 2 (below) give the vibrational frequencies and

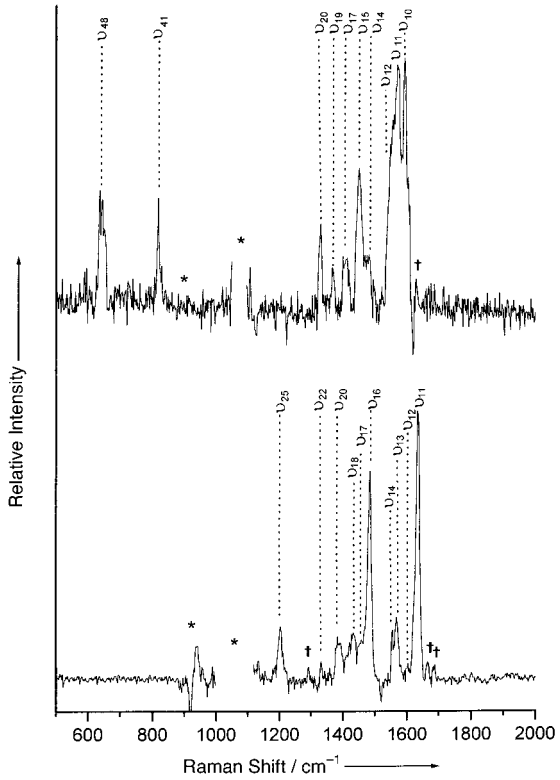

Figure 1. Transient 416 nm resonance Raman spectrum of 2-fluorenylnitrene (top) obtained after 309 nm photolysis of 2-fluorenylnitrene in acetonitrile. Transient 416 nm resonance Raman spectrum of the 2-fluorenylnitrenium ion (bottom) obtained after 309 nm photolysis of 2-fluorenylnitrene in a 75 % water/25 % acetonitrile (by volume) mixed solvent. The transient Raman spectra were found by subtracting a probe-only spectrum and a pump-only spectrum from a pump/probe spectrum to remove solvent and precursor Raman bands. Both spectra were obtained with a pump/probe time delay of 10 ns. The asterisks mark solvent subtraction artifacts and the daggers mark small stray light or ambient light artifacts. The tentative vibrational assignments for some of the Raman bands are labeled (refer to text and Tables 1 and 2 for more details).

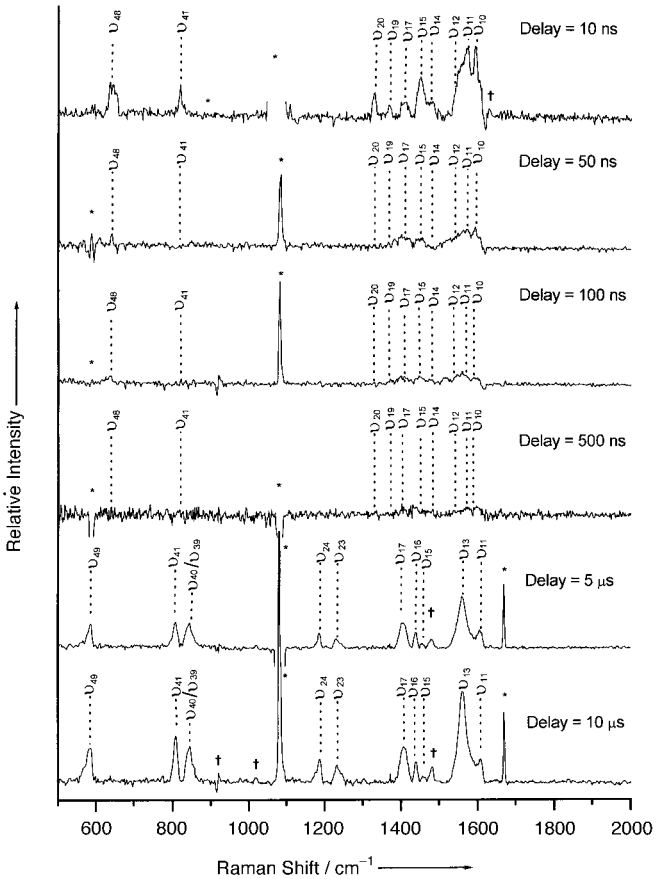

Figure 2. Time-resolved resonance Raman spectra obtained after 309 nm photolysis of 2-fluorenylnitrene in acetonitrile. The time-resolved resonance Raman spectra were found by subtracting probe-only spectra and pump-only spectra from pump/probe spectra to remove solvent and precursor Raman bands. The spectra were obtained with different pump/probe time delays (10, ns, 50 ns, 100 ns, 500 ns, 5 μs, and 10 μs) as indicated next to each spectrum. The asterisks mark solvent subtraction artifacts and the daggers mark small stray light or ambient light artifacts. The tentative vibrational assignments for some of the Raman bands are labeled (refer to text and Tables 1 and 2 for more details).

tentative assignments for the Raman bands observed in the transient and time-resolved resonance Raman spectra in acetonitrile (Figures 1 and 2). Inspection of Figure 1 shows that the transient Raman spectrum recorded in acetonitrile is very different than that obtained in a 75 % water/25 % acetonitrile (by volume) solvent system. This indicates that two distinctly different species are formed on the 10 ns timescale after photolysis of 2-fluorenylnitrene in the two different solvents. We have previously shown that the transient resonance Raman spectrum acquired in the 75 % water/25 % acetonitrile solvent system is caused by the singlet 2-fluorenylnitrenium ion species (the reader is referred to ref. [60] for more details). Several different groups have attributed the formation of singlet arylnitrenium ions follow-

  0947-6539/02/0809-2164 $ 20.00+.50/0 *Chem. Eur. J.* **2002**, *8*, No. 9

ing photolysis of aryl azides to be caused by a fast protonation reaction of the singlet arylnitrene species initially produced in the presence of water.[31–37, 40] Such a protonation reaction would be expected to be substantially slower in a pure acetonitrile and it is tempting to assign the transient Raman spectrum observed in the top of Figure 1 to the singlet and/or the triplet 2-fluorenylnitrene species. Comparison of the 10 ns, 50 ns, and 100 ns spectra with the 5 μs and 10 μs spectra shown in Figure 2 reveals that a new species is formed on the microsecond timescale from the initially produced 2-fluorenylnitrene.

Several studies have used a comparison of vibrational frequencies computed with density functional to experimental frequencies observed in either time-resolved Raman or IR spectra to convincingly assign several different arylnitrenium ions to their singlet ground states,[48, 56, 60] and we expect a similar approach may be useful for arylnitrene species. We have performed UBPW91/cc-PVDZ calculations to find the optimized geometry and predicted vibrational frequencies for the singlet and triplet 2-fluorenylnitrene species. Figure 3 shows selected parameters for the optimized geometry of the singlet and triplet 2-fluorenylnitrene species (a more complete listing of the geometry parameters can be found in the Supporting Information). Tables 1 and 2 compare the UBPW91/cc-PVDZ-computed vibrational frequencies to the experimental Raman values. We note that the experimental Raman bands in the time-resolved resonance Raman spectra observed on the 10–100 ns and 5–10 μs timescales in Figure 2 provide a reasonable fingerprint for the transient species produced after photolysis of the 2-fluorenylnitrene precursor in acetonitrile. Examination of Tables 1 and 2 show that there is generally good agreement between the calculated and experimental frequencies. The calculated vibrational frequencies of triplet and singlet 2-fluorenylnitrene differ by $\approx 10\ cm^{-1}$ and $11\ cm^{-1}$, respectively, on average from the ten experimental Raman bands for the species observed in the 10 ns (and in the 50 ns and 100 ns) spectra listed in Table 1. The Raman bands observed in the time-resolved resonance Raman spectra of Figure 2 cannot clearly distinguish whether the spectra are mainly attributed to the triplet and/or singlet states of 2-fluorenylnitrene. However, there is other evidence that the experimental spectra on the 10–100 ns timescale are probably mostly caused by the singlet 2-fluorenylnitrene species.

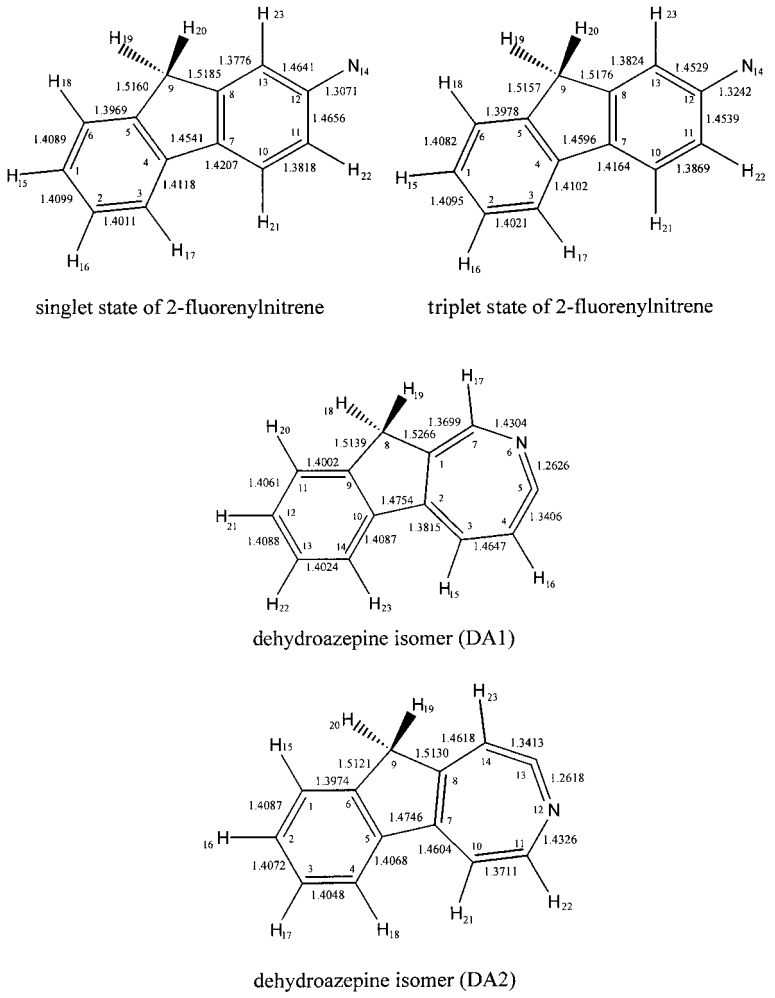

Figure 3. Schematic diagrams of the triplet and singlet states of 2-fluorenylnitrene and the two isomers of the dehydroazepine product species (DA1 and DA2) with the atoms numbered. The numbering of the atoms corresponds to those in the Supporting Information for the UBPW91/cc-PVDZ and BPW91/cc-PVDZ calculations. Selected geometry parameters (bond lengths [Å]) are indicated in the diagrams.

The electronic configurations and geometric structures of phenylnitrene (PhN) in its low-lying electronic states have been intensively investigated experimentally and theoretically by Platz, Borden, Karney, and co-workers.[7, 8, 18, 20, 21, 42–46, 52–54] The open-shell triplet state was confirmed to be a ground state ($^3A_2$) of PhN with the open-shell singlet state ($^1A_2$) located $\approx 18\ kcal\,mol^{-1}$ above the ground state.[8, 21, 61] The $^3A_2$ state has two unpaired electrons partitioned into two nonbonding orbitals and are mostly localized on the nitrogen atom, while the in the $^1A_2$ state, one of the singly occupied orbitals is delocalized into the phenyl ring and this significantly stabilizes the $^1A_2$ state so that the energy differences between the two states is much smaller for PhN than that found for NH. We obtained similar results for the triplet and singlet states of 2-fluorenylnitrene from our UBPW91/cc-PVDZ calculations. The triplet state is lower in energy than the open-shell singlet state by $\approx 7.4\ kcal\,mol^{-1}$ for the 2-fluorenylnitrene species and this singlet–triplet splitting is much lower than that found for PhN. This is due in large part to the larger conjugation system in 2-fluorenylnitrene relative to PhN. The UBPW91-calculated spin densities show that the two unpaired electrons are mainly located on the N atom with little of the charge delocalized

Table 1. Experimental Raman vibrational frequencies observed in the time-resolved resonance Raman spectra of 2-fluorenylnitrene and its dehydroazepine product(s) shown in Figure 1 and Figure 2.[a] The experimental vibrational frequencies are compared to those from UBPW91/cc-PVDZ computations for the singlet and triplet states of 2-fluorenylnitrene species observed in the 10 ns, 50 ns and 100 ns time-resolved resonance Raman spectra (see text for more details).

Triplet 2-fluorenylnitrene		Singlet 2-fluorenylnitrene		Experiment
vibrational mode approx. description	UBPW91/cc-PVDZ calcd. value [cm^{-1}]	vibrational mode approx. description	UBPW91/cc-PVDZ calcd. value [cm^{-1}]	10 ns time-resolved Raman frequency shift [cm^{-1}]
$\tilde{\nu}_{50}$, ring def.	527	$\tilde{\nu}_{51}$, ring def.	524	
$\tilde{\nu}_{49}$, ring def.	563	$\tilde{\nu}_{50}$, CCC bend	563	
$\tilde{\nu}_{48}$, CCC bend	571	$\tilde{\nu}_{49}$, ring def.	567	
$\tilde{\nu}_{49}$, ring def.	**634**	**$\tilde{\nu}_{48}$, CCC bend**	**623**	**637**
$\tilde{\nu}_{46}$, ring def.	692	$\tilde{\nu}_{47}$, ring def.	690	
$\tilde{\nu}_{45}$, ring def.	719	$\tilde{\nu}_{46}$, CCC bend	709	
$\tilde{\nu}_{44}$, ring def. + C–H bend	724	$\tilde{\nu}_{45}$, C–H bend (o.p.[b])	722	
$\tilde{\nu}_{43}$, C–H bend	767	$\tilde{\nu}_{44}$, CCC bend	738	
$\tilde{\nu}_{42}$, C–H bend	**805**	$\tilde{\nu}_{43}$, C–H bend	766	
$\tilde{\nu}_{41}$, ring def.	**806**	$\tilde{\nu}_{42}$, ring def. + C–H bend	798	
$\tilde{\nu}_{40}$, C–H bend + CH_2 bend	839	**$\tilde{\nu}_{41}$, CCC bend**	**814**	**818**
$\tilde{\nu}_{39}$, C–H bend	853	$\tilde{\nu}_{40}$, C–H bend (o.p.)	835	
$\tilde{\nu}_{38}$, ring def.	894	$\tilde{\nu}_{39}$, C–H bend	850	
$\tilde{\nu}_{37}$, C–H bend + CH_2 bend	908	$\tilde{\nu}_{38}$, ring def.	885	
$\tilde{\nu}_{36}$, C–H bend	935	$\tilde{\nu}_{37}$, ring def.	907	
$\tilde{\nu}_{35}$, ring 1 C–H bend	941	$\tilde{\nu}_{36}$, ring def. + C–H bend	934	
$\tilde{\nu}_{34}$, ring 2 C–H bend	965	$\tilde{\nu}_{35}$, C–H bend (o.p.)	941	
$\tilde{\nu}_{33}$, ring def.	980	$\tilde{\nu}_{34}$, C–H bend (o.p.)	964	
$\tilde{\nu}_{32}$, C–H bend	999	$\tilde{\nu}_{33}$, CCC bend	980	
$\tilde{\nu}_{31}$, C–H bend	1069	$\tilde{\nu}_{32}$, ring 3 C–C stretch	1021	
$\tilde{\nu}_{30}$, C–H bend	1098	$\tilde{\nu}_{31}$, C–H bend	1078	
$\tilde{\nu}_{29}$, CH_2 twist	1112	$\tilde{\nu}_{30}$, C–H bend	1102	
$\tilde{\nu}_{28}$, C–H bend + CH_2 scissor	1124	$\tilde{\nu}_{29}$, CH_2 twist	1114	
$\tilde{\nu}_{27}$, C–H bend	1135	$\tilde{\nu}_{28}$, ring def. + C–H bend	1121	
$\tilde{\nu}_{26}$, C–H bend + CH_2 wag	1165	$\tilde{\nu}_{27}$, ring def. + C–H bend	1141	
$\tilde{\nu}_{25}$, C–H bend	1183	$\tilde{\nu}_{26}$, C–H bend + CH_2 wag	1165	
$\tilde{\nu}_{24}$, C–H bend	1202	$\tilde{\nu}_{25}$, ring def. + C–H bend	1183	
$\tilde{\nu}_{23}$, C–H bend	1233	$\tilde{\nu}_{24}$, ring def. + C–H bend	1202	
$\tilde{\nu}_{22}$, C–H bend	1278	$\tilde{\nu}_{23}$, C–C stretch	1221	
$\tilde{\nu}_{21}$, C–C stretch + C–H bend	1294	$\tilde{\nu}_{22}$, C–H bend + CH_2 wag	1276	
$\tilde{\nu}_{20}$, ring 1 C–N stretch + C–C stretch	**1327**	$\tilde{\nu}_{21}$, C–C stretch	1296	
$\tilde{\nu}_{19}$, CH_2 rock + C–H bend	**1364**	**$\tilde{\nu}_{20}$, C–C stretch + CH_2 scissor**	**1352**	**1331**
$\tilde{\nu}_{18}$, CH_2 twist	1375	**$\tilde{\nu}_{19}$, C–C stretch + CH_2 scissor**	**1371**	**1367**
$\tilde{\nu}_{17}$, C–C stretch	**1395?**	$\tilde{\nu}_{18}$, C–C stretch + CH_2 scissor	1377	
$\tilde{\nu}_{16}$, C–C stretch + C–H bend	**1437?**	**$\tilde{\nu}_{17}$, C–C stretch + N–H stretch**	**1429**	**1410**
$\tilde{\nu}_{15}$, C–C stretch + C–H bend	**1448**	**$\tilde{\nu}_{16}$, C–C stretch + C–C_2 scissor**	**1431**	
$\tilde{\nu}_{14}$, C–C stretch + C–H bend	**1468**	**$\tilde{\nu}_{15}$, C–C stretch**	**1453**	**1451**
$\tilde{\nu}_{13}$, C–C stretch	1503	**$\tilde{\nu}_{14}$, C–C stretch + C–N stretch**	**1475**	**1479**
$\tilde{\nu}_{12}$, C–C stretch	**1577**	$\tilde{\nu}_{13}$, C–C stretch	1495	
$\tilde{\nu}_{11}$, C–C stretch	**1578**	**$\tilde{\nu}_{12}$, C–C stretch**	**1575**	**1551**
$\tilde{\nu}_{10}$, ring 2, C–C stretch	**1605**	**$\tilde{\nu}_{11}$, C–C stretch + N–H stretch**	**1579**	**1573**
		$\tilde{\nu}_{10}$, C–C stretch	**1604**	**1591**

[a] Possible vibrational band assignments are also shown based on comparison with calculated vibrational frequencies from UBPW91/cc-PVDZ or BPW91/cc-PVDZ computations in the 500 – 1700 cm^{-1} fingerprint region for the ground singlet and triplet state of 2-fluorenylnitrene and the ground singlet state of the two isomers of the dehydroazepine products (see text). [b] o.p. = out-of-plane.

into the N-bonded phenyl ring for the triplet state, while the spin density on the N atom is less than one for the open-shell singlet state with a noticeable amount of spin density located on the C1, C3, C5, C7, C10, C11, and C13 atoms. It is evident that one electron is mainly distributed into the σ orbital of the N atom and the other is in the π orbital that is delocalized into the phenyl rings for the open-shell singlet state of 2-fluorenylnitrene. This leads to noticeable differences in the geometry of the two states, as shown in Tables 1 and 2. For example, the C12–N14 bond length is 1.3071 Å in the singlet state and 1.3242 Å in the triplet state. Similarly, the C–C alternation pattern is noticeably different in the singlet and triplet states, as shown in Figure 3. These geometry differences do give rise to a number of differences in some of the vibrational frequencies (see Table 1); however, the ten resonance Raman bands observed are not particularly diagnostic for distinguishing between the triplet and singlet state 2-fluorenylnitrene species.

We note that singlet 2,6-dicyanophenylnitrene was found to have a transient absorption at ≈405 nm with a lifetime of ≈2 ns in room temperature solutions.[57] This is consistent with our observation of the 2-fluorenylnitrene species with a 416 nm probe wavelength. In addition, it was found that *para* substitution of the phenyl nitrene with a cyano group raised the barrier to the cyclization pathway and noticeably increased the singlet *p*-cyanophenylnitrene lifetime to ≈8 ns.[57]

  0947-6539/02/0809-2166 $ 20.00+.50/0 *Chem. Eur. J.* **2002**, *8*, No. 9

Table 2. Experimental Raman vibrational frequencies observed in the time-resolved resonance Raman spectra of 2-fluorenylnitrene and its dehydroazepine product(s) shown in Figures 1 and 2.[a] The experimental vibrational frequencies are compared to those from UBPW91/cc-PVDZ computations for the two isomers of the dehydroazepine 2-fluorenyl derivatives observed in the 5 μs and 10 μs time-resolved resonance Raman spectra (see text for more details).

Isomer 1 of 2-fluorenyl dehydroazepine		Isomer 2 of 2-fluorenyl dehydroazepine		Experiment
vibrational mode approx. description	BPW91/cc-PVDZ calcd. value [cm^{-1}]	vibrational mode approx. description	BPW91/cc-PVDZ calcd. value [cm^{-1}]	5 μs time-resolved Raman freq. shift [cm^{-1}]
$\tilde{\nu}_{52}$, ring def.	503	$\tilde{\nu}_{51}$, ring def.	518	
$\tilde{\nu}_{51}$, ring def. + C=C=N bend	517	$\tilde{\nu}_{50}$, ring def.	552	
$\tilde{\nu}_{50}$, ring def. + C=C=N bend	537	**$\tilde{\nu}_{49}$, ring def. + C=C=N bend**	**565**	**586**
$\tilde{\nu}_{49}$, CCC bend	**591**	$\tilde{\nu}_{48}$, ring def.	617	
$\tilde{\nu}_{48}$, ring def.	621	$\tilde{\nu}_{47}$, ring def.	646	
$\tilde{\nu}_{47}$, ring def.	652	$\tilde{\nu}_{46}$, CCC bend	684	
$\tilde{\nu}_{46}$, ring def.	677	$\tilde{\nu}_{45}$, ring def.	691	
$\tilde{\nu}_{45}$, ring def.	698	$\tilde{\nu}_{44}$, C–H bend (o.p.[b])	715	
$\tilde{\nu}_{44}$, C–H bend (o.p.)	720	$\tilde{\nu}_{43}$, CCC bend + C–H bend (o.p.)	748	
$\tilde{\nu}_{43}$, ring def.	728	$\tilde{\nu}_{42}$, C–H bend (o.p.)	760	
$\tilde{\nu}_{42}$, C–H bend (o.p.)	761	**$\tilde{\nu}_{41}$, CCC bend**	**814**	**808**
$\tilde{\nu}_{41}$, CCC bend	**814**	$\tilde{\nu}_{40}$, ring def.	830	
$\tilde{\nu}_{40}$, ring def.	**838**	**$\tilde{\nu}_{39}$, C–C bend (o.p.) + CH_2 rock**	**845**	**844**
$\tilde{\nu}_{39}$, C–H bend + CH_2 rock	850	$\tilde{\nu}_{38}$, ring def. + CH_2 rock	887	
$\tilde{\nu}_{38}$, ring 1 C–H bend (o.p.)	866	$\tilde{\nu}_{37}$, ring def. + C–H bend	909	
$\tilde{\nu}_{37}$, C–H bend (o.p.) + CH_2 rock	910	$\tilde{\nu}_{36}$, ring def. + C–H bend	925	
$\tilde{\nu}_{36}$, C–H bend (o.p.)	935	$\tilde{\nu}_{35}$, CCC bend	948	
$\tilde{\nu}_{35}$, CCC bend	945	$\tilde{\nu}_{34}$, ring def.	970	
$\tilde{\nu}_{34}$, C–H bend (o.p.)	963			
$\tilde{\nu}_{33}$, C–N stretch	1000	$\tilde{\nu}_{33}$, CCC bend + C=C–N bend	970	
$\tilde{\nu}_{32}$, ring 3 CC stretch	1025	$\tilde{\nu}_{32}$, ring def.	1023	
$\tilde{\nu}_{31}$, ring 1 CC stretch	1037	$\tilde{\nu}_{31}$, ring def.	1055	
$\tilde{\nu}_{30}$, ring def. + C–H bend	1085	$\tilde{\nu}_{30}$, ring def. + C–H bend	1088	
$\tilde{\nu}_{29}$, CC stretch + C–N stretch	1099	$\tilde{\nu}_{29}$, ring def. + CH_2 twist	1094	
$\tilde{\nu}_{28}$, CH_2 twist	1120	$\tilde{\nu}_{28}$, C–C stretch	1111	
$\tilde{\nu}_{27}$, C–C stretch + C–H bend	1133	$\tilde{\nu}_{27}$, C–H bend + CH_2 wag	1124	
$\tilde{\nu}_{26}$, C–H bend	1142	$\tilde{\nu}_{26}$, C–H bend	1142	
$\tilde{\nu}_{25}$, ring 2 and 3 C–C stretch	1172	$\tilde{\nu}_{25}$, C–H bend	1177	
$\tilde{\nu}_{24}$, CH_2 wag + C–H bend	**1185**	**$\tilde{\nu}_{24}$, C–C stretch**	**1182**	**1188**
$\tilde{\nu}_{23}$, C–C stretch	**1228**	**$\tilde{\nu}_{23}$, C–H bend**	**1215**	**1231**
$\tilde{\nu}_{22}$, C–C stretch	1260	$\tilde{\nu}_{22}$, C–C stretch	1260	
$\tilde{\nu}_{21}$, C–H bend	1275	$\tilde{\nu}_{21}$, C–C stretch + C–H bend	1278	
$\tilde{\nu}_{20}$, ring 1 C–C stretch	1300	$\tilde{\nu}_{20}$, C–C stretch	1330	
$\tilde{\nu}_{19}$, C–C stretch	1334	$\tilde{\nu}_{19}$, CH_2 scissor	1355	
$\tilde{\nu}_{18}$, ring 3 C–C stretch	1373	$\tilde{\nu}_{18}$, C–C stretch + C–N stretch	1372	
$\tilde{\nu}_{17}$, CH_2 scissor	**1390**	**$\tilde{\nu}_{17}$, C–C stretch**	**1383**	**1407**
$\tilde{\nu}_{16}$, ring 3 C–C stretch	**1452**	**$\tilde{\nu}_{16}$, C–C stretch**	**1443**	**1439**
$\tilde{\nu}_{15}$, ring 3 C–C stretch	**1454**	**$\tilde{\nu}_{15}$, C–C stretch**	**1452**	**1457**
$\tilde{\nu}_{14}$, C–C stretch ring 1 and 2	1548	$\tilde{\nu}_{14}$, C–C stretch	1512	
$\tilde{\nu}_{13}$, C–C stretch	**1570**	**$\tilde{\nu}_{13}$, C–C stretch**	**1556**	**1560**
$\tilde{\nu}_{12}$, C–C stretch	1588	$\tilde{\nu}_{12}$, C–C stretch	1587	
$\tilde{\nu}_{11}$, C–C stretch ring 3	**1611**	**$\tilde{\nu}_{11}$, C–C stretch ring 3**	**1612**	**1608**
$\tilde{\nu}_{10}$, N=C=C asym. stretch	1887	$\tilde{\nu}_{10}$, N=C=C asym. stretch	1891	

[a] Possible vibrational band assignments are also shown based on comparison with calculated vibrational frequencies from UBPW91/cc-PVDZ or BPW91/cc-PVDZ computations in the 500–1700 cm^{-1} fingerprint region for the ground singlet and triplet state of 2-fluorenylnitrene and the ground singlet state of the two isomers of the dehydroazepine products (see text). [b] o.p. = out-of-plane.

One could reasonably expect that *para* substitution with a phenyl ring may also stabilize the singlet arylnitrene species and increase its lifetime significantly. Our results indicate that this is probably the case with the 2-fluorenylnitrene species with the UBPW91/cc-PVDZ calculations predicting a substantial stabilization of the singlet state to produce a gap between the singlet and triplet states of only 7.4 kcal mol^{-1} compared to ≈18 kcal mol^{-1} for PhN. Therefore, it is probable that the singlet 2-fluorenylnitrene species is readily observed on the 10–100 ns timescale after photolysis of the azide precursor in acetonitrile. This is consistent with the approximate 30–50 ns lifetime of the 2-fluorenylnitrene species observed in the time-resolved resonance Raman spectra of Figure 2. The fact that the transient species observed in acetonitrile is readily quenched by water to form the corresponding singlet nitrenium ion provides further support for our assignment and indicates the singlet 2-fluorenylnitrene species has a lifetime that is sufficiently long to enable it to easily react with water.

It is important to consider the product formed at longer times from the 2-fluorenylnitrene species and observed in the 5 and 10 μs spectra shown in Figure 2. Singlet arylnitrenes, such as PhN, tend to react and form ring-expansion dehydroazepine products, while triplet nitrenes, such as PhN, tend to form azo dimerization products with an N=N group in the condensed phase.[3–9] Resonance Raman spectra have been

obtained for a number of azo compounds with phenyl groups (such as *trans*-azobenzene, 4-nitro,4′-dimethylamino-azobenzene, and others) and these resonance Raman spectra typically have most of their intensity in Raman bands associated with the N=N chromophore and corresponding vibrational modes in the $\nu = 1400 - 1500\ cm^{-1}$ region with moderate intensity in bands above $1500\ cm^{-1}$ associated with aromatic C=C bonds.[62–65] This is in contrast with the resonance Raman intensity pattern observed in the 5 μs and 10 μs time-resolved resonance Raman spectra shown in Figure 2, in which most of the Raman intensity is in the $1560 - 1610\ cm^{-1}$ region of the C=C-stretch vibrational modes and only moderate intensity in the $1400 - 1500\ cm^{-1}$ region. Thus, it is not likely that the species observed in the 5 and 10 μs spectra are caused by an azo dimerization compound with a N=N chromophore. Dehydroazepine products have been previously observed after photolysis of other aryl azides by means of time-resolved IR spectroscopy.[14, 15] Therefore, we performed some BPW91/cc-PVDZ computations to obtain the optimized geometry and vibrational frequencies for two isomers of the dehydroazepine products (DA1 and DA2) that can be formed from 2-fluorenylnitrene. The lower part of Figure 3 shows schematic diagrams (and selected optimized geometry parameters) of DA1 and DA2 with their atoms numbered as used in Table 2, which also lists the vibrational frequencies computed at the BPW91/cc-PVDZ level. There is reasonable agreement between the ten experimental Raman vibrational band frequencies observed in the 5 μs and 10 μs spectra of Figure 2 and those computed for the two dehydroazepine species (DA1 and DA2). The difference between the experimental and theoretical values are approximately $7\ cm^{-1}$ and $9\ cm^{-1}$ for DA1 and DA2, respectively. The level of agreement is similar for both the closely related dehydroazepine ring-expansion product species, and our current Raman spectra cannot clearly distinguish between them or indicate the relative branching ratio for the formation of the two dehydroazepine species. However, it is clear that dehydroazepine ring-expansion products are formed on the microsecond timescale (5 and 10 μs spectra) from the 2-fluorenylnitrene species. Since ring-expansion dehydroazepine products or intermediates are associated with singlet arylnitrenes, this suggests that the time-resolved resonance Raman spectra on the nanosecond timescale observed in Figure 1 are mainly from the singlet 2-fluorenylnitrene species.

It is intriguing that the 2-fluorenylnitrene species first decreases in intensity without any apparent immediate formation of the dehydroazepine species or other species. This indicates the presence of another intermediate that does not absorb very well at the wavelength of the 416 nm probe. The identity of this dark intermediate is most probably an azirine species formed from the singlet 2-fluorenylnitrene. We note that formation of azo dimerization products from triplet state arylnitrenes does not involve any intermediate step. This, the decay behavior of the 2-fluorenylnitrene species, and the formation of the dehydroazepine species in the spectra shown in Figure 2 provide further support for our assignment of the 2-fluorenylnitrene nanosecond spectra to be caused by the singlet state species. An elegant study by Morawietz and Sander[38] demonstrated the formation of fluorinated azirine intermediates from fluorinated phenyl nitrenes in low-temperature matrices by means of IR and UV/Vis absorption spectroscopy to detect the azirine species. They found that the azirines had a noticeable absorption band at ≈250 nm with little absorption in the 350 – 450 nm region. This is consistent with both the time-resolved resonance Raman spectra shown in Figure 2 and the possibility of the dark intermediate derived from an azirine intermediate formed from the singlet 2-fluorenylnitrene and then reacting further to produce the dehydroazepine species observed on the microsecond timescale.

Examination of the simple schematics of the normal mode descriptions for the vibrational bands experimentally observed in Figure 2 (see Figures S1 and S2 in the Supporting Information) indicates that the normal mode descriptions are somewhat complicated with contributions from a number of different internal coordinates for each mode. Therefore, it is helpful to make use of the predicted geometry of the UBPW91/cc-PVDZ and BPW91/cc-PVDZ computational results in order to elucidate the degree to which the observed Raman band frequencies correlate with the structure and bond order of the 2-fluorenylnitrene and the two isomers of the dehydroazepine ring-expansion species. Selected optimized structural parameters from the UBPW91/cc-PVDZ and BPW91/cc-PVDZ calculations are shown in Figure 3 and a more complete listing is given in the Supporting Information.

Inspection of the bond lengths in Figure 3 reveals that the C–N bond lengths are reasonably short and there is noticeable alternation in the C–C bond lengths in the phenyl rings for both the triplet and singlet 2-fluorenylnitrene species. The C–N bond length is very similar in both the singlet 2-fluorenylnitrene species (1.3071 Å) and the 2-fluorenylnitrenium ion (1.3077 Å), while the triplet 2-fluorenylnitrene is noticeably longer (1.3242 Å). These C–N bond lengths are closer to that for a typical C=N bond (≈1.28 Å) than a C–N bond (≈1.40 Å).[66] These short C–N bonds and the alternation of the C–C bond lengths in the phenyl rings observed for the 2-fluorenylnitrene species indicates both the singlet and triplet states have significant iminocyclohexadienyl character, although to a varying extent. This behavior is similar to that found for several arylnitrenium ions[48, 56, 60] including the 2-fluorenylnitrenium ion.[60]

Symmetric aromatic C=C stretch vibrational modes in the $1568 - 1628\ cm^{-1}$ region were previously found to correlate with the degree of iminocyclohexadienyl character of several arylnitrenium ions.[48, 56, 60] Comparison of similar modes in 2-fluorenylnitrene indicates this kind of correlation for arylnitrene species is not as clear and appears to be complicated by the nature of the nitrene moiety. For example, the singlet and triplet 2-fluorenylnitrenes have very similar vibrational frequencies of the C=C stretch mode (1575, 1579, and $1604\ cm^{-1}$ for the singlet state and 1577, 1578, and $1605\ cm^{-1}$ for the triplet state) although the aromatic C–C and C–N bonds are noticeably different in the optimized geometries shown in Figure 3. This is probably partly caused by the complex and by the delocalized nature of the vibrational normal modes that are not clearly associated with

  0947-6539/02/0809-2168 $ 20.00+.50/0 *Chem. Eur. J.* **2002**, *8*, No. 9

mainly one or the other carbon atom rings as was the case for the singlet 2-fluorenylnitrenium ion and some other singlet arylnitrenium ions.[56, 60]

It is very interesting to compare the optimized geometry of the singlet 2-fluorenylnitrene species to the singlet 2-fluorenylnitrenium ion species (see Table 2 of Ref. [60]). Addition of a proton to singlet 2-fluorenylnitrene to form the singlet 2-fluorenylnitrenium ion[60] results in little change in the C–N bond (from 1.3071 Å in the nitrene to 1.3077 Å in the nitrenium ion). However, formation of the nitrenium ion from the nitrene leads to noticeably stronger alternation of the C–C bonds in the two phenyl rings. The first phenyl ring (to which the nitrogen atom is attached) has differences in the C–C bond alternation for the C11–C12 and C11–C10 bonds of 0.0838 Å in the nitrene and 0.1031 Å in the nitrenium ion. There are similar changes for the C12–C13 and C8–C13 bonds of 0.0865 Å in the nitrene and 0.1011 Å for the nitrenium ion, the C7–C10 and C10–C11 bonds of $\approx$0.0389 Å in the nitrene and 0.0672 Å for the nitrenium ion, and for the C7–C8 and C8–C13 bonds of 0.0589 Å in the nitrene and 0.0812 Å for the nitrenium ion. There are also significant increases in the C–C bond alternation pattern in the other phenyl ring as the singlet 2-fluorenylnitrene becomes a singlet 2-fluorenylnitrenium ion. For example, the change in the C3–C4 and C2–C3 bonds in the nitrene is 0.0107 Å and 0.0323 Å in the nitrenium ion; between the C4–C5 and C5–C6 bonds it is 0.030 Å for the nitrene and 0.04553 Å for the nitrenium ion; between the C1–C2 and the C2–C3 bonds it is 0.0088 Å for the nitrene and 0.0295 Å for the ion; between the C1–C6 and C5–C6 bonds it is 0.0120 Å for the nitrene and 0.0135 Å for the nitrenium ion. Our results indicate that the cyclohexadienyl character and charge delocalization into the phenyl rings becomes substantially stronger upon protonation of the 2-fluorenylnitrene species to produce the 2-fluorenylnitrenium ion accompanied by little change in the C–N bond length. The singlet 2-fluorenylnitrene species appears to have a lifetime in the order of approximately 30–50 ns (see Figure 2), while the singlet 2-fluorenylnitrenium ion has a substantially longer lifetime, namely on the microsecond timescale.[31] There appears to be an interesting correlation of the degree of cyclohexadienyl character and charge delocalization into the two phenyl rings with the lifetime of the 2-fluorenylnitrene and 2-fluorenylnitrenium ion species. Our results also indicate that the nitrenium ion moiety enables substantially better charge delocalization into the phenyl rings than the neutral nitrene moiety for similar imine character of the C–N bond.

We have demonstrated the utility of time-resolved resonance Raman spectroscopy to examine chemical intermediates, such as nitrenes and dehydroazepines produced after photolysis of azido compounds such as 2-fluorenylnitrene. The spectra obtained from resonance Raman spectroscopy have enhancement of Raman band intensities for the species involved in the transient electronic absorption spectra. Thus, the resonance Raman vibrational frequencies are correlated with and are indicative of the transient absorption spectra. This enables characterization of different species, even though their transient absorption spectra are very similar to one another. To make improved vibrational assignments of the time-resolved resonance Raman spectra for the nitrene and dehydroazepine chemical intermediates, it will be useful to obtain spectra for isotopic derivatives some time in the future. Since Raman and IR absorption are complementary techniques, it would also be useful to characterize the intermediates with time-resolved IR absorption spectroscopy to more fully characterize the vibrational frequencies and to compare them to predictions from ab initio or density functional computations.

Conclusion

We have obtained time-resolved resonance Raman spectra of several species formed on the nanosecond and microsecond timescales after UV photolysis of a solution of 2-fluorenylnitrene in acetonitrile. The species observed in the nanosecond timescale spectra (10 ns, 50 ns, and 100 ns) had ten Raman vibrational bands whose frequencies are in reasonable agreement with those from UBPW91/cc-PVDZ calculations for the singlet and triplet states of 2-fluorenylnitrene. Both the singlet and triplet states of 2-fluorenylnitrene have significant iminocyclohexadienyl character, similar to arylnitrenium ions. The species observed on the microsecond timescale (5 and 10 μs) spectra had ten Raman vibrational bands whose frequencies are in reasonable agreement with those from BPW91/cc-PVDZ calculations for two isomers of dehydroazepine products formed from 2-fluorenylnitrenes. Since dehydroazepine products are typically associated with their formation from singlet arylnitrenes, this suggests that most of the Raman intensity in the 2-fluorenylnitrene nanosecond timescale spectra is caused by the singlet 2-fluorenylnitrene species. The UBPW91/cc-PVDZ computations indicate that the singlet 2-fluorenylnitrene species is significantly stabilized relative to the triplet state so that there is only a gap of 7.4 kcal mol^{-1} between the singlet and triplet states compared to the singlet–triplet gap of $\approx$18 kcal mol^{-1} in phenylnitrenes. The significantly smaller singlet–triplet gap for 2-fluorenylnitrenes and the quenching of 2-fluorenylnitrene by water to give the singlet 2-fluorenylnitrenium ion are both consistent with our assignment of the nanosecond timescale resonance Raman spectra to the singlet 2-fluorenylnitrene species. As the 2-fluorenylnitrene species decays, there is no immediate formation of the dehydroazepine product. This suggests that a dark intermediate species is first produced from the 2-fluorenylnitrene species before the dehydroazepine species is produced, and it is probable that this dark intermediate is an azirine. Related azirines were previously observed by others in low-temperature matrices and these species had significant absorption at $\approx$250 nm but not in the 350–450 nm region near to the 416 nm probe wavelength used in our time-resolved resonance Raman experiments. This is consistent with the hypothesis of an azirine species being the dark intermediate formed as the 2-fluorenylnitrene decays and the azirine then decays to produce dehydroazepine products.

Comparison of our results for the singlet 2-fluorenylnitrene species with that previously found for the singlet 2-fluorenylnitrenium ion species reveals that the cyclohexadienyl character and charge delocalization into the phenyl rings becomes

substantially stronger when the 2-fluorenylnitrene species is protonated to form the 2-fluorenylnitrenium ion. However, the C–N bond length is about the same in both species. There is a correlation of the degree of cyclohexadienyl character and charge delocalization into the two phenyl rings of the singlet 2-fluorenylnitrene (lifetime of ≈30–50 ns) and 2-fluorenylnitrenium ion (microsecond scale lifetime) species with their lifetimes. However, it is probably more important that the ground state of the nitrenium ion is the singlet state and, hence, it has a longer lifetime since it cannot decay by intersystem crossing to another state.

Experimental Section

Synthesis of the 2-fluorenylnitrene: 2-Fluorenylnitrene was prepared by means of a previously reported method for the synthesis of azido compounds.[67] In a 200 mL round-bottom flask, 2-aminofluorene (1.81 g, 10 mmol) was dissolved in water (40 mL) that contained concentrated sulfuric acid (10 mL). This solution was cooled to below 5 °C in an ice bath and diazotized with a solution of $NaNO_2$ (0.76 g, 11 mmol) in distilled water (7 mL). The mixture was stirred in an ice bath for 1 h with occasional addition of small portions of water to rinse the walls of the flask. A solution of NaN_3 (1.34 g, 20 mmol) in water (10 mL) was added at 0 °C. After 10 min, water (70–80 mL) was added at 0 °C, and the resulting suspension was filtered to isolate the product (≈1.56 g). The product was then purified by recrystallization from ethanol. ^{1}H NMR (500 MHz, $CDCl_3$): $\delta = 7.73$ (d, $J = 8.0$ Hz, 2H), 7.52 (d, $J = 7.4$ Hz, 1H), 7.38 (t, $J = 7.4$ Hz, 1H), 7.29 (m, 1H), 7.21 (s, 1H), 7.02 (m, 1H), 3.89 (s, 2H); IR (film): $\tilde{\nu} = 2113$, 1604, 1581, 1454, 1401, 1307, 1292, 1281, 838, 766, 732 cm^{-1}; MS (EI): *m*/*z* (%): 179 (100) [$C_{13}H_9N^+$], 152 (24), 111 (27), 97 (45), 85 (53), 77 (73), 71 (58). **Caution**: The azide precursor compound, 2-fluorenylnitrene, is potentially explosive (especially if allowed to dry) and should be handled with care.

Computational methods: The density functional calculations made use of the Gaussian program suite[68] with complete geometry optimization. Vibrational frequency calculations were performed analytically with the UBPW91 or BPW91 methods[69, 70] and the cc-PVDZ basis set[71] for the singlet and triplet states of 2-fluorenylnitrene and the two dehydroazepine product species (DA1 and DA2). The Supporting Information lists the computed geometry parameters and vibrational frequencies for the singlet and triplet 2-fluorenylnitrene species and the two dehydroazepine product (DA1 and DA2) species from selected parts of the Gaussian output files.

Transient and time-resolved resonance Raman spectroscopy experiments: The 2-fluorenylnitrene precursor was prepared with concentrations in the 2–5 mM range in acetonitrile for the transient resonance Raman experiments that led to the observation of the singlet 2-fluorenylnitrene and dehydroazepine species. Additional experiments were carried out with ≈5 mM 2-fluorenylnitrene in a 75% water/25% acetonitrile (by volume) mixed solvent system with a 2 mM acetate buffer and a pH of 3.5 in order to quench the singlet 2-fluorenylnitrene species to produce the singlet 2-fluorenylnitrenium ion reaction product.[60]

The transient resonance Raman and time-resolved resonance Raman apparatus and experimental methods have been described elsewhere and only a brief account will be provided here.[60, 72–76] The hydrogen Raman-shifted laser lines produced from the harmonics of a nanosecond-pulsed Nd:YAG laser system provided the pump (309 nm) and probe (416 nm) excitation wavelengths for the transient and time-resolved resonance Raman experiments. The transient resonance Raman experiments used optical time-delays of 0–10 ns between the pump and probe laser beams. The time-resolved resonance Raman experiments employed two Nd:YAG lasers electronically synchronized to each other by means of a pulse delay generator (Stanford Research Systems model DG-535) to control the relative timing of the two lasers (both the firing of the lamp and Q-switch pulses) Two fast photodiodes, whose output was displayed on a 500 MHz oscilloscope (Hewlett Packard 54522A), were used to examine the relative timing of the pump and probe laser pulses. The jitter between the pump and probe pulses was observed to be < 5 ns. In both types of resonance Raman experiments the laser beams were lightly focused onto a flowing liquid stream of sample with a near-collinear geometry. The scattered Raman light was collected by means of reflective optics and a backscattering geometry to minimize the effects of chromatic aberration and sample reabsorption of the light. The collected scattered Raman light was imaged through a polarization scramble mounted on the entrance slit of a 0.5 m spectrograph whose grating then dispersed the Raman signal onto a CCD detector cooled with liquid nitrogen. The Raman signal was acquired by the CCD for approximately 300 to 600 s before being read out to an interfaced PC computer. About 10 to 20 of these readouts were summed to obtain a resonance Raman spectrum. Pump-only, probe-only, and pump/probe resonance Raman spectra were acquired. A background scan was also recorded. The known Raman bands of acetonitrile were used to calibrate the wavenumber shifts of the resonance Raman spectra. The solvent and precursor Raman bands were removed by subtracting the probe-only spectrum from the pump/probe spectrum. The pump-only spectrum and the background spectrum were also subtracted from the pump/probe spectrum to obtain the transient resonance Raman spectrum.

Acknowledgements

This work was supported by grants from the Committee on Research and Conference Grants (CRCG), the Research Grants Council (RGC) of Hong Kong (HKU 7112/00P), and the Large Items of Equipment Allocation 1993–94, from the University of Hong Kong.

[1] E. F. V. Scriven in *Reactive Intermediates, Vol. 2* (Ed.: R. A. Abramovich), Plenum, New York, **1982**, Chapter 1.
[2] C. Wentrup, *Reactive Molecules*, Wiley-Interscience, New York, **1984**, Chapter 4.
[3] M. S. Platz in *Azides and Nitrenes: Reactivity and Utility* (Ed.: E. F. V. Scriven), Academic, New York, **1984**, Chapter 7.
[4] M. S. Platz, V. M. Maloney in *Kinetics and Spectroscopy of Carbenes and Biradicals* (Ed.: M. S. Platz) Plenum, New York, **1990**, pp. 303–320.
[5] M. S. Platz, E. Leyva, K. Haider, *Org. Photochem.* **1991**, *11*, 367–398.
[6] G. B. Schuster, M. S. Platz, *Adv. Photochem.* **1992**, *17*, 69–143.
[7] M. S. Platz, *Acc. Chem. Res.* **1995**, *28*, 487–492.
[8] W. T. Borden, N. P. Gritsan, C. M. Hadad, W. L. Karney, C. R. Kemnitz, M. S. Platz, *Acc. Chem. Res.* **2000**, *33*, 765–771.
[9] A. K. Schrock, G. B. Schuster, *J. Am. Chem. Soc.* **1984**, *106*, 5228–5234.
[10] T. Donnelly, I. R. Dunkin, D. S. D. Norwood, A. Prentice, C. J. Shields, P. C. P. Thomson, *J. Chem. Soc. Perkin Trans. 2* **1985**, 307–310.
[11] I. R. Dunkin, T. Donnelly, T. S. Lockhart, *Tetrahedron Lett.* **1985**, *26*, 359–362.
[12] E. Leyva, M. S. Platz, *Tetrahedron Lett.* **1985**, *26*, 2147–2150.
[13] E. Leyva, M. S. Platz, G. Persy, J. Wirz, *J. Am. Chem. Soc.* **1986**, *108*, 3783–3790.
[14] C. J. Shields, D. R. Chrisope, G. B. Schuster, A. J. Dixon, M. Poliakoff, J. J. Turner, *J. Am. Chem. Soc.* **1987**, *109*, 4723–4726.
[15] Y.-Z. Li, J. P. Kirby, M. W. George, M. Poliakoff, G. B. Schuster, *J. Am. Chem. Soc.* **1988**, *110*, 8092–8098.
[16] R. Poe, J. Grayzar, M. J. T. Young, E. Leyva, K. Schnapp, M. S. Platz, *J. Am. Chem. Soc.* **1991**, *113*, 3209–3211.
[17] M. J. T. Young, M. S. Platz, *J. Org. Chem.* **1991**, *56*, 6403–6406.
[18] R. Poe, K. Schnapp, M. J. T. Young, J. Grayzar, M. S. Platz, *J. Am. Chem. Soc.* **1992**, *114*, 5054–5067.
[19] C. G. Younger, R. A. Bell, *J. Chem. Soc. Chem. Commun.* **1992**, 1359–1361.
[20] S.-J. Kim, T. P. Hamilton, H. F. Schaefer, *J. Am. Chem. Soc.* **1992**, *114*, 5349–5355.
[21] D. A. Hrovat, E. E. Waali, W. T. Borden, *J. Am. Chem. Soc.* **1992**, *114*, 8698–8699.
[22] A. Marcinek, M. S. Platz, *J. Phys. Chem.* **1993**, *97*, 12674–12677.
[23] A. Marcinek, E. Leyva, D. Whitt, M. S. Platz, *J. Am. Chem. Soc.* **1993**, *115*, 8609–8612.

  0947-6539/02/0809-2170 $ 20.00+.50/0

[24] K. A. Schnapp, R. Poe, E. Leyva, N. Soundarajan, M. S. Platz, *Bioconjugate Chem.* **1993**, *4*, 172–177.
[25] K. A. Schnapp, M. S. Platz, *Bioconjugate Chem.* **1993**, *4*, 178–183.
[26] G. B. Anderson, D. E. Falvey, *J. Am. Chem. Soc.* **1993**, *115*, 9870–9871.
[27] T. Ohana, M. Kaise, S. Nimura, O. Kikuchi, A. Yabe, *Chem. Lett.* **1993**, 765–768.
[28] P. A. Davidse, M. J. Kahley, R. A. McClelland, M. Novak, *J. Am. Chem. Soc.* **1994**, *116*, 4513–4514.
[29] A. Marcinek, M. S. Platz, Y. S. Chan, R. Floresca, K. Rajagopalan, M. Golinski, D. Watt, *J. Phys. Chem.* **1994**, *98*, 412–419.
[30] K. Lamara, A. D. Redhouse, R. K. Smalley, J. R. Thompson, *Tetrahedron* **1994**, *50*, 5515–5526.
[31] R. A. McClelland, P. A. Davidse, G. Haczialic, *J. Am. Chem. Soc.* **1995**, *117*, 4173–4174.
[32] R. J. Robbins, L. L.-N. Yang, G. B. Anderson, D. E. Falvey, *J. Am. Chem. Soc.* **1995**, *117*, 6544–6552.
[33] S. Srivastava, D. E. Falvey, *J. Am. Chem. Soc.* **1995**, *117*, 10186–10193.
[34] R. A. McClelland, M. J. Kahley, P. A. Davidse, *J. Phys. Org. Chem.* **1996**, *9*, 355–360.
[35] R. A. McClelland, M. J. Kahley, P. A. Davidse, G. Hadzialic, *J. Am. Chem. Soc.* **1996**, *118*, 4794–4803.
[36] R. J. Robbins, D. M. Laman, D. E. Falvey, *J. Am. Chem. Soc.* **1996**, *118*, 8127–8135.
[37] R. J. Moran, D. E. Falvey, *J. Am. Chem. Soc.* **1996**, *118*, 8965–8966.
[38] J. Morawietz, W. Sander, *J. Org. Chem.* **1996**, *61*, 4351–4354.
[39] O. Castell, V. M. Garcia, C. Bo, R. Caballol, *J. Comput. Chem.* **1996**, *17*, 42–48.
[40] J. Michalak, H. B. Zhai, M. S. Platz, *J. Phys. Chem.* **1996**, *100*, 14028–14036.
[41] X.-Z. Sun, I. G. Virrels, M. W. George, H. Tomioka, *Chem. Lett.* **1996**, 1089–1090.
[42] W. L. Karney, W. T. Borden, *J. Am. Chem. Soc.* **1997**, *119*, 1378–1387.
[43] W. L. Karney, W. T. Borden, *J. Am. Chem. Soc.* **1997**, *119*, 3347–3350.
[44] N. P. Gritsan, T. Yuzawa, M. S. Platz, *J. Am. Chem. Soc.* **1997**, *119*, 5059–5060.
[45] R. Born, C. Burda, P. Senn, J. Wirz, *J. Am. Chem. Soc.* **1997**, *119*, 5061–5062.
[46] N. P. Gritsan, H. B. Zhai, T. Yuzawa, D. Karweik, J. Brooke, M. S. Platz, *J. Phys. Chem. A* **1997**, *101*, 2833–2840.
[47] R. J. Moran, D. E. Falvey, *J. Am. Chem. Soc.* **1996**, *118*, 8965–8966.
[48] S. Srivastava, J. P. Toscano, R. J. Moran, D. E. Falvey, *J. Am. Chem. Soc.* **1997**, *119*, 11552–11553.
[49] E. Leyva, R. Sagredo, *Tetrahedron* **1998**, *54*, 7367–7374.
[50] A. Nicolaides, H. Tomioka, S. Murata, *J. Am. Chem. Soc.* **1998**, *120*, 11530–11531.
[51] A. Nicolaides, T. Naakayama, K. Yamazaki, H. Tomioka, S. Koseki, L. L. Stracener, R. J. McMahon, *J. Am. Chem. Soc.* **1999**, *121*, 10563–10572.
[52] N. P. Gritsan, Z. Zhu, C. M. Hadad, M. S. Platz, *J. Am. Chem. Soc.* **1999**, *121*, 1202–1207.
[53] N. P. Gritsan, A. Gudmundsdottir, D. Tigelaar, M. S. Platz, *J. Phys. Chem. A* **1999**, *103*, 3458–3461.
[54] N. P. Gritsan, D. Tigelaar, M. S. Platz, *J. Phys. Chem. A* **1999**, *103*, 4465–4469.
[55] M. Cerro-Lopez, N. P. Gritsan, Z. Zhu, M. S. Platz, *J. Phys. Chem. A* **2000**, *104*, 9681–9686.
[56] S. Srivastava, P. H. Ruane, J. P. Toscano, M. B. Sullivan, C. J. Cramer, D. Chiapperino, E. C. Reed, D. E. Falvey, *J. Am. Chem. Soc.* **2000**, *122*, 8271–8278.
[57] N. P. Gritsan, I. Likhotvorik, M.-L. Tsao, N. Celebi, M. S. Platz, W. L. Karney, C. R. Kemnitz, W. T. Borden, *J. Am. Chem. Soc.* **2001**, *123*, 1425–1433.
[58] H. Inui, S. Murata, *Chem. Lett.* **2001**, 832–833.
[59] A. Nicolaides, T. Enyo, D. Miura, H. Tomioka, *J. Am. Chem. Soc.* **2001**, *123*, 2628–2636.
[60] P. Zhu, S. Y. Ong, P. Y. Chan, K. H. Leung, D. L. Phillips, *J. Am. Chem. Soc.* **2001**, *123*, 2645–2649.
[61] R. N. McDonald, S. J. Davidson, *J. Am. Chem. Soc.* **1993**, *115*, 10857–10862.
[62] N. Biswas, S. Umapathy, *Chem. Phys. Lett.* **1995**, *236*, 24–29.
[63] N. Biswas, S. Umapathy, *J. Chem. Phys.* **1997**, *107*, 7849–7858.
[64] N. Biswas, S. Umapathy, *Chem. Phys. Lett.* **1998**, *294*, 181–190.
[65] T. Fujino, T. Tahara, *J. Phys. Chem. A* **2000**, *104*, 4203–4210.
[66] J. March, *Advanced Organic Chemistry*, 2nd ed., McGraw-Hill, New York, **1977**.
[67] a) B. R. Brown, L. W. Yielding, W. E. White, Jr., *Mutat. Res.* **1980**, *70*, 17–27; b) W. E. White, Jr., L. W. Yielding in *Methods in Enzymology Vol. XLVI Affinity Labeling* (Eds.: W. B. Jakoby, M. Wilchek), Academic Press, Orlando, Florida, **1977**, pp. 646–647.
[68] Gaussian 98 (Revision A.7), M. J. Frisch, G. W. Trucks, H. B. Schlegel, G. E. Scuseria, M. A. Robb, J. R. Cheeseman, V. G. Zakrzewski, J. A. Montgomery, Jr., R. E. Stratmann, J. C. Burant, S. Dapprich, J. M. Millam, A. D. Daniels, K. N. Kudin, M. C. Strain, O. Farkas, J. Tomasi, V. Barone, M. Cossi, R. Cammi, B. Mennucci, C. Pomelli, C. Adamo, S. Clifford, J. Ochterski, G. A. Petersson, P. Y. Ayala, Q. Cui, K. Morokuma, D. K. Malick, A. D. Rabuck, K. Raghavachari, J. B. Foresman, J. Cioslowski, J. V. Ortiz, A. G. Baboul, B. B. Stefanov, G. Liu, A. Liashenko, P. Piskorz, I. Komaromi, R. Gomperts, R. L. Martin, D. J. Fox, T. Keith, M. A. Al-Laham, C. Y. Peng, A. Nanayakkara, C. Gonzalez, M. Challacombe, P. M. W. Gill, B. Johnson, W. Chen, M. W. Wong, J. L. Andres, C. Gonzalez, M. Head-Gordon, E. S. Replogle, J. A. Pople, Gaussian, Inc., Pittsburgh PA, **1998**.
[69] A. Becke, *J. Chem. Phys.* **1986**, *84*, 4524–4529.
[70] J. P. Perdew, K. Burke, Y. Wang, *Phys. Rev. B* **1996**, *54*, 16533–16539.
[71] T. H. Dunning, *J. Chem. Phys.* **1989**, *90*, 1007–1023.
[72] L. C. T. Shoute, D.-H. Pan, D. L. Phillips, *Chem. Phys. Lett.* **1998**, *290*, 24–28.
[73] D.-H. Pan, D. L. Phillips, *J. Phys. Chem. A* **1999**, *103*, 4737–4743.
[74] X. Zheng, D. L. Phillips, *J. Phys. Chem. A* **2000**, *104*, 6880–6886.
[75] X. Zheng, D. L. Phillips, *J. Chem. Phys.* **2000**, *113*, 3194–3203.
[76] X. Zheng, C. W. Lee, Y.-L. Li, W.-H. Fang, D. L. Phillips, *J. Chem. Phys.* **2001**, *114*, 8347–8356.

Received: September 27, 2001 [F3579]